

Electronic Supplementary Material

Plasmon-enhanced magneto-optical detection of single-molecule magnets

Francesco Pineider^{1,2*}, *Esteban Pedrueza Villalmanzo*³, *Michele Serri*², *Addis Mekonnen Adamu*^{3,4},
*Evgeniya Smetanina*³, *Valentina Bonanni*², *Giulio Campo*², *Lorenzo Poggini*², *Matteo Mannini*²,
*César de Julián Fernández*⁵, *Claudio Sangregorio*^{6,2}, *Massimo Gurioli*⁷, *Alexandre Dmitriev*³,
*Roberta Sessoli*²

1 Department of Chemistry and Industrial Chemistry & INSTM, University of Pisa, Pisa, Italy

*francesco.pineider@unipi.it

2 Department of Chemistry ‘Ugo Schiff’ & INSTM, University of Florence, Sesto Fiorentino (FI),
Italy

3 Department of Physics, University of Gothenburg, Göteborg, Sweden

4 Department of Physics, Bahir Dar University, Bahir Dar, Ethiopia

5 CNR-IMEM, Parma, Italy

6 CNR-ICCOM, Florence, Italy

7 Department of Physics and Astronomy, University of Florence, Sesto Fiorentino (FI), Italy

Fitting of the optical extinction spectra. The extinction spectrum of **AuDisks** was fitted using a Gaussian peak for the interband transition edge and two Lorentzian peaks for the plasmonic component; the second Lorentzian, at higher energy and with ~25% amplitude with respect to the main resonance is required to properly fit the experimental spectrum, and it probably arises from a subset of lower aspect ratio disks (*i.e.* same diameter, thicker disks), as found from AFM characterization. The result of the fit is shown in Figure S4a. The Q band spectral region of **TbPc₂** was fitted with a Lorentzian and a Gaussian component; the result is shown in Figure S5a.

In order to fit the extinction spectrum of **TbPc₂@Au**, a total of 5 peak functions were used: a Gaussian profile for the Au interband transition edge, with fixed peak position and width with respect to the one used to fit **AuDisks**, two Lorentzian oscillators, whose relative peak distance was fixed to the value found for **AuDisks** for the plasmonic component. The molecular component was fitted using a Lorentzian function and a Gaussian function, as done for **TbPc₂**. The result is shown in Figure S5b.

Fitting of the plasmonic component of the MCD spectra. While the MCD line shape originated by **TbPc₂** is complex and its modelling is not straightforward without an in-depth study of the frontier orbitals of the molecule, the plasmonic contribution to the MCD spectrum is easily reproduced as the difference of two shifted circular magnetoplasmonic peaks. Following an approach used to evaluate field-induced exciton splitting in quantum dots¹ and dilute magnetic quantum dots,² we fitted the MCD spectrum of **AuDisks** as the difference of two energy shifted LSPR peaks, leaving ΔE as the free parameter. The line profile was taken as two couples of Lorentzian functions, whose peak position and amplitude parameters were fixed from the fit of the optical spectrum. Peak width was allowed to vary to take into account the fact that optical extinction was measured at room temperature, while MCD was acquired at 1.5 K: as expected, peak width decreased (~5%). The second free parameter was the peak splitting. Results are shown in Figure S4b. The contribution of interband transitions is negligible in MCD, so the Gaussian component of the extinction spectrum does not appear in the MCD fitting routine. The fit yielded $\Delta E = 0.11$ meV at 5 T, coherently with the cyclotron frequency value and with the model we developed previously.³

For sample **TbPc₂@Au**, the same procedure was carried out *i.e.* peak position and amplitude were taken from the fit of the extinction spectrum, while peak width and splitting were left as free parameters. In this case, however, the data interval on which the fit was carried out was restricted to the spectral area dominated by the plasmonic component, *i.e.* the 1.2 – 1.7 eV photon energy range. The full plasmonic contribution was then extrapolated over the remaining energy range. The energy shift was estimated to be $\Delta E = 0.10$ meV at 5 T in good agreement with that of plain **AuDisks**.

Estimate of the extinction of the TbPc₂ layer evaporated on detuned gold nanoantennas. Considering the extinction intensity of the TbPc₂ layer evaporated on glass (Figure S6), we estimate that the thickness of the molecular layer is approximately ~1 nm. The weak shoulder due to the TbPc₂ on detuned nanodisks cannot be directly fitted because its intensity is very low, due to the absence of plasmonic enhancement and it is comparable to the error made by fitting the LSPR peak. We then devised the following strategy: we fitted the extinction spectra of the pristine detuned gold disks and of the disks with a TbPc₂ layer, using only plasmonic components in both cases. In the latter case, the residual of the fitting showed a clear signature of the TbPc₂ layer, together with other oscillations. Oscillations were partly removed by subtracting the residuals of the fitting of pristine gold disks, yielding the blue trace in Figure S6b. Comparison with the absorption of TbPc₂ on glass (green trace, same figure), allows us concluding that the intensities of the molecular peaks are analogous, within the limitations of the method. This confirms that the enhancement we observed in the on-resonance sample is of plasmonic origin.

Estimate of the detection limit of the present MCD setup in terms of TbPc₂ monolayers. The noise level of the MCD setup employed in this study is $\Delta(\text{Extinction})_n = 1.10^{-5}$, expressed as the standard deviation of the MCD signal in the working conditions (in differential extinction units). We can define a limit of detection of a magneto-optical signal as $\text{LOD} = 3. \Delta(\text{Extinction})_n = 3.10^{-5}$.⁴ The signal arising from 2 nm TbPc₂ on a glass substrate is around 1.10^{-4} , so the setup is in principle able to detect magneto-optical signals from TbPc₂ layers of effective thickness $d = 0.6$ nm, corresponding to approximately half a monolayer of standing molecules. Considering the amplification factor ~ 5 arising from plasmonic enhancement, which increases the MCD signal from the same layer thickness to 6.10^{-4} , the estimated LOD falls to 0.1 nm, corresponding to less than 0.1 monolayers of TbPc₂.

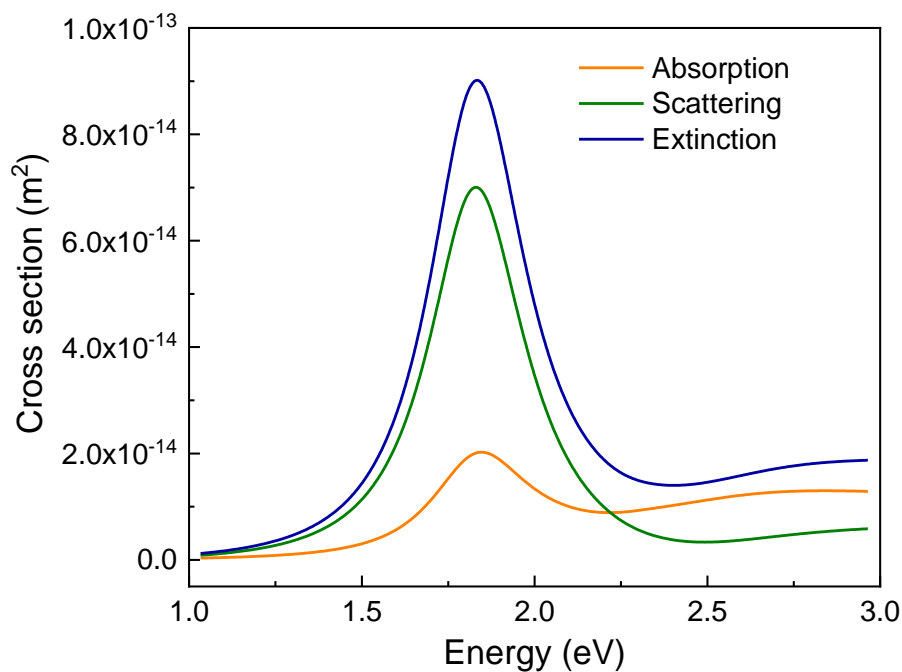


Figure S1: Calculated absorption and scattering contributions and their sum (=extinction) to the cross section of a single gold nanodisk with similar geometry to those used in the experiment.

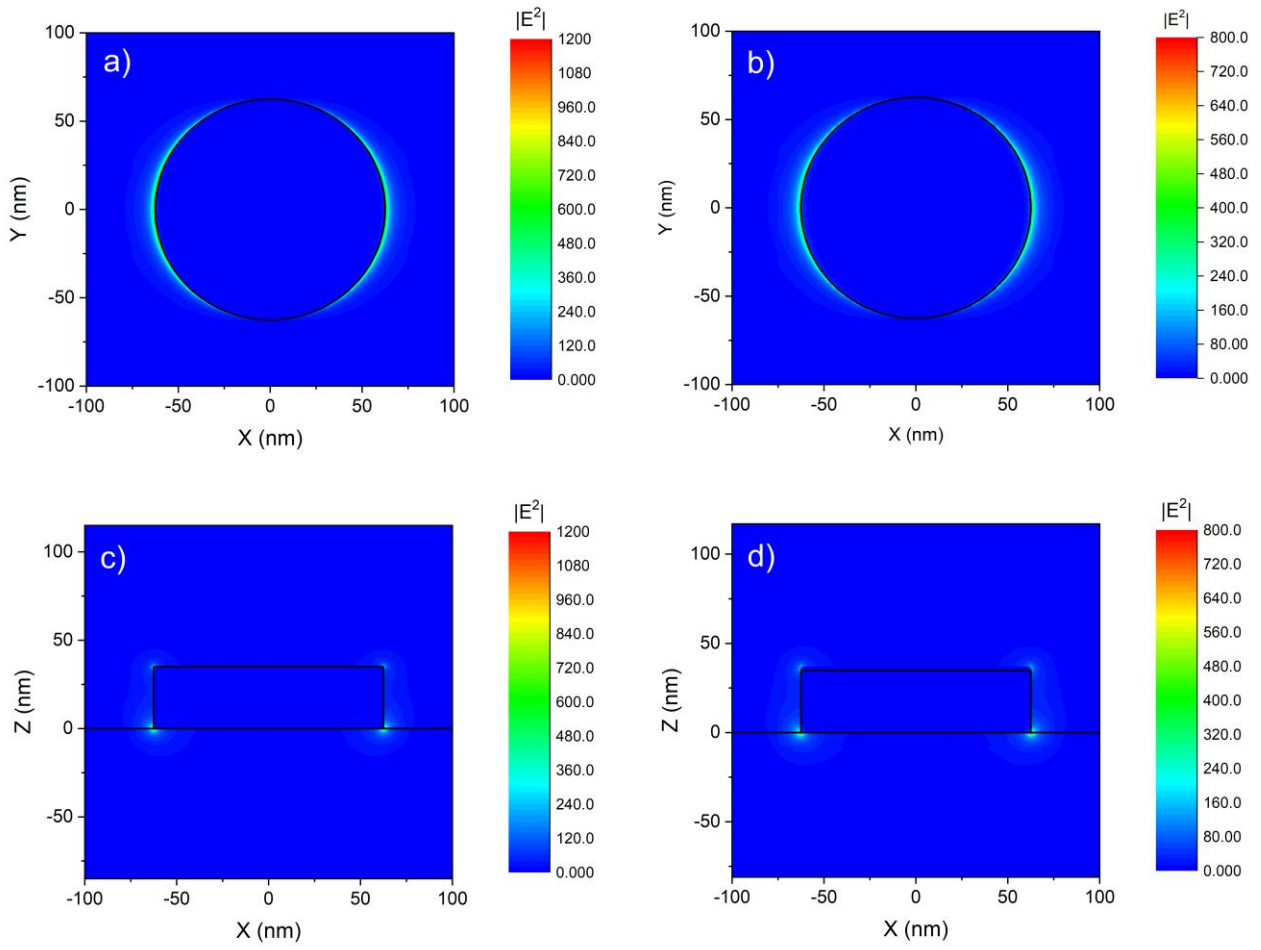


Figure S2: Squared near field distributions of **AuDisks** (a: top view, c: side view) and **TbPc₂@Au** (b: top view, d: side view) at LSPR peak. For top views, monitor was positioned at the base of the antenna; for side views, crossing the antenna.

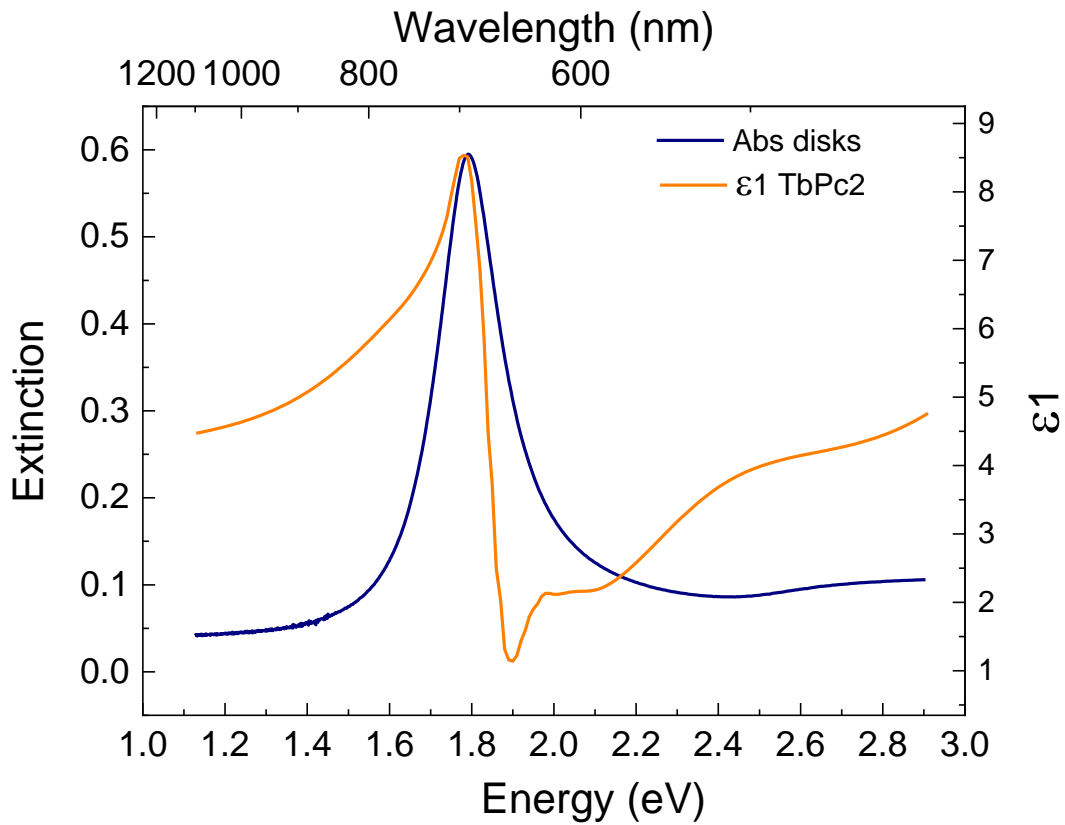


Figure S3: Comparison between LSPR position in **AuDisks** and the real part (ϵ_1) of the complex dielectric function of a TbPc₂ film (data for the latter from ref.⁵).

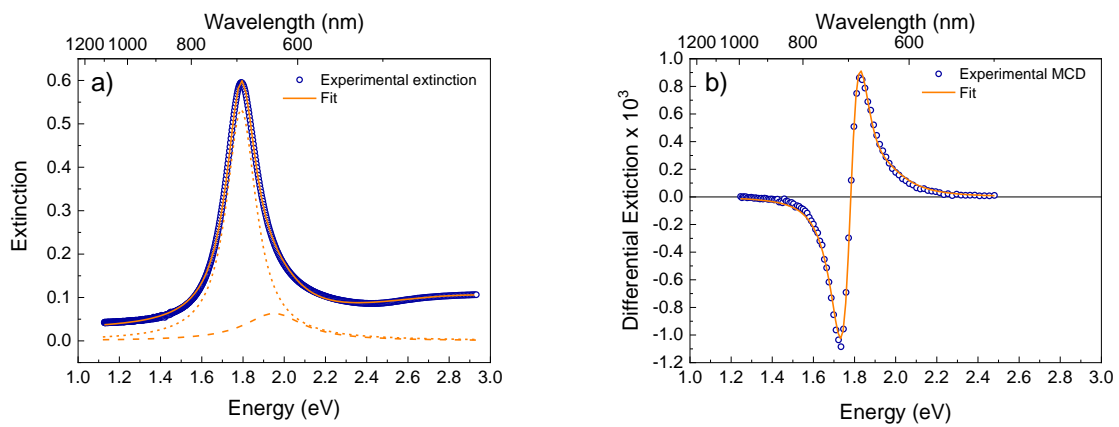


Figure S4: Fitting of a) the extinction spectrum and b) MCD spectrum of **AuDisks**.

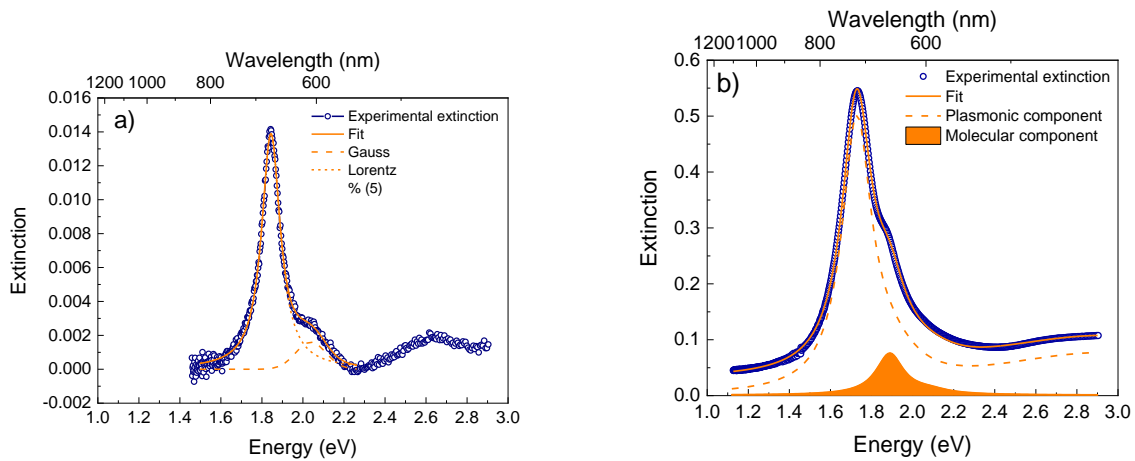


Figure S5: Fitting of the extinction spectra of a) TbPc₂ and b) TbPc₂@Au.

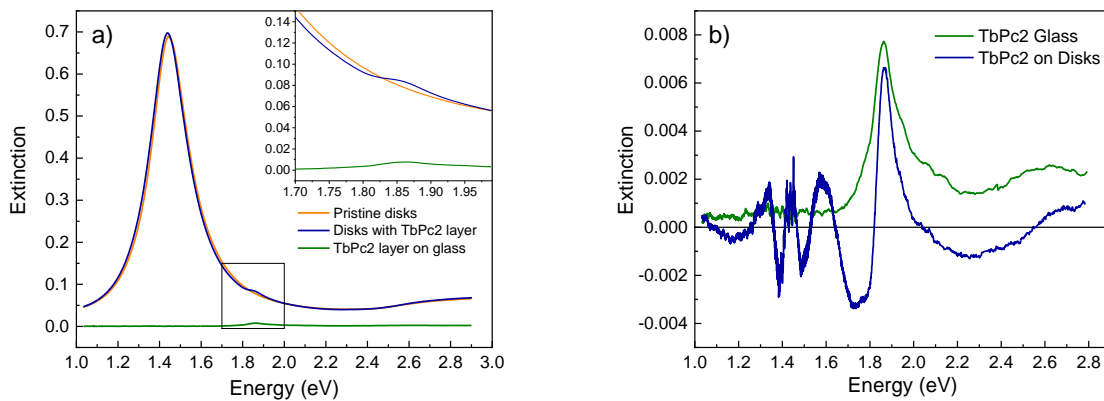


Figure S6: a) Extinction spectra of pristine detuned gold nanoantennas (orange), the same disks with a thin evaporated layer of TbPc₂ (blue) and a TbPc₂ film of the same thickness co-deposited on a glass substrate (green). Inset shows the magnified area of the TbPc₂ resonance for all three spectra. b) Comparison of the extinction from the TbPc₂ deposit on glass (green) and the TbPc₂ contribution in the extinction spectrum of TbPc₂ evaporated on disks (blue). The latter was calculated as the difference of the residuals obtained by fitting the extinction spectra of the pristine disks and the disks with a TbPc₂ layer.

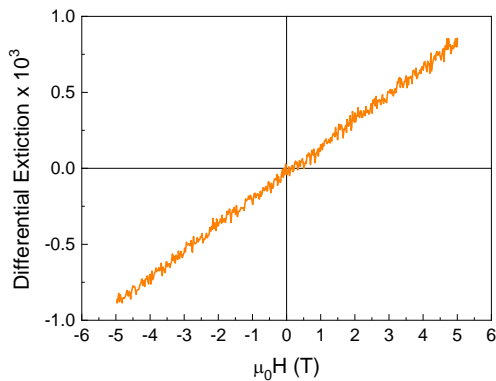


Figure S7: MCD field dependence of AuDisks measured at E = 1.82 eV and T = 1.5 K.

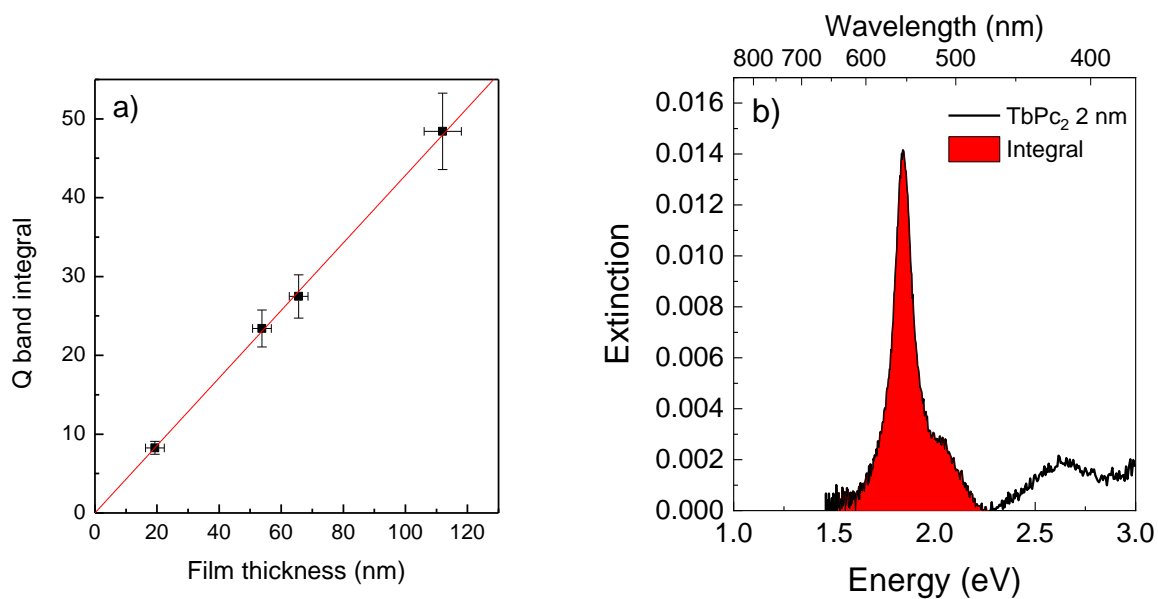


Figure S8: a) Extinction vs thickness calibration curve for TbPc₂ on glass. Extinction intensity was measured as the integral of the Q band of the complex. b) Integral of the extinction over the Q band region used to estimate the thickness of the 2 nm TbPc₂ film on glass.

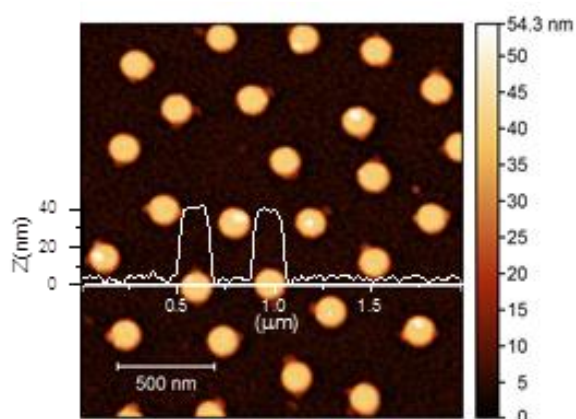


Figure S9: AFM topography image of TbPc₂@Au, showing the height profile measured along the horizontal axis.

References

1. Kuno, M.; Nirmal, M.; Bawendi, M.; Efros, A.; Rosen, M., Magnetic circular dichroism study of CdSe quantum dots. *The Journal of Chemical Physics* **1998**, *108* (10), 4242-4247.
2. Archer, P. I.; Santangelo, S. A.; Gamelin, D. R., Direct observation of sp-d exchange interactions in colloidal Mn²⁺-and Co²⁺-doped CdSe quantum dots. *Nano letters* **2007**, *7* (4), 1037-1043.
3. Pineider, F.; Campo, G.; Bonanni, V.; Fernandez Cde, J.; Mattei, G.; Caneschi, A.; Gatteschi, D.; Sangregorio, C., Circular magnetoplasmonic modes in gold nanoparticles. *Nano Letters* **2013**, *13* (10), 4785-9
4. Chen, S.; Svedendahl, M.; Käll, M.; Gunnarsson, L.; Dmitriev, A., Ultrahigh sensitivity made simple: nanoplasmonic label-free biosensing with an extremely low limit-of-detection for bacterial and cancer diagnostics. *Nanotechnology* **2009**, *20*, 434015.
5. Robaschik, P.; Fronk, M.; Toader, M.; Klyatskaya, S.; Ganss, F.; Siles, P. F.; Schmidt, O. G.; Albrecht, M.; Hietschold, M.; Ruben, M., Tuning the magneto-optical response of TbPc 2 single molecule magnets by the choice of the substrate. *Journal of Materials Chemistry C* **2015**, *3* (31), 8039-8049.